

Delay time and Non-Adiabatic Calibration of the Attoclock

Multiphoton process versus tunneling in strong field interaction

Ossama Kullie

Theoretical Physics, Institute for Physics, Department of Mathematics and Natural Science, University of Kassel, Germany*

Abstract

The measurement of the tunneling time in attosecond experiments, termed attoclock, offers a fruitful opportunity to understand the role of time in quantum mechanics. It has triggered a hot debate about the tunneling time and the separation into two regimes or processes of different character, the multiphoton ionization and the tunneling (field) ionization. In the present work, we show that our tunneling model explains the nonadiabatic effects (photon absorption) as well. Again, as it was the case in the adiabatic field calibration, we reach a very good agreement with the experimental data in the nonadiabatic field calibration of Hofmann et al (J. of Mod. Opt. **66**, 1052, 2019). Interestingly, our model offers a clear picture for the multiphoton and tunneling parts. In particular, the tunneling part is now compensated mainly by the absorption of a number photons that is characteristic for the barrier height. The well known separation of multiphoton and tunneling regimes (usually by Keldysh parameter) is clarified with a more advanced picture. Surprisingly, at a field strength $F < F_a$ (the atomic field strength), the model indicates always a delay time with respect to the quantum limit, that is the ionization time at F_a where the barrier suppression ionization sets up.

Keywords: Ultrafast science, attosecond physics, tunneling and ionization time delay, nonadiabatic effects, time-energy uncertainty relation, time and time-operator in quantum mechanics.

A. Introduction

In previous works we presented a tunneling model, in which the tunneling time (T-time) is a delay time with respect to ionization time at atomic field strength F_a . Our tunneling time is impressively in good agreement with the attoclock result or the attosecond (angular streaking) experiment of Landsmann et al [1–3] for He-atom [4], and Sainadh et al [5] for Hydrogen atom [6] (apart from a factor 1/2). Furthermore, our tunneling time picture [4] shows an intriguing similarity to the famous Bohr-Einstein weighing *photon box Gedanken experiment (BE-photon-box-GE)* [7], [8] (p. 132), where the former can be seen as a realization of the later.

Our simple tunneling model was introduced in [4] (see fig 1). In the model an electron can be ionized by a laser pulse with an electric field strength (hereafter field strength) F , where a direct ionization happen when the field strength reaches a threshold called atomic field strength $F_a = I_p^2/(4Z_{eff})$ [9, 10], where I_p is the ionization potential of the system (atom or molecule) and Z_{eff} is the effective nuclear charge in the single-active electron approximation. However, for $F < F_a$ the ionization can happen by tunneling mechanism, through a barrier, which is built by an effective potential due

to the Coulomb potential of the nucleus and the electric field of the laser pulse. It can be expressed in a one-dimensional form

$$V_{eff}(x) = V(x) - xF = -\frac{Z_{eff}}{x} - xF, \quad (1)$$

compare fig 1. In the model the tunneling process can be described solely by the ionization potential I_p of the valence (the interacting) electron and the peak field strength F , which leads to the quantity $\delta_z = \sqrt{I_p^2 - 4Z_{eff}F}$, where F stands (throughout this work) for *the peak electric field strength at maximum*. In fig 1 (for details see [4]), the inner (entrance $x_{e,-}$) and outer (exit $x_{e,+}$) points are given by $x_{e,\pm} = (I_p \pm \delta_z)/(2F)$, the barrier width $d_B = x_{e,+} - x_{e,-} = \delta_z/F$, and the barrier height (at $x_m(F) = \sqrt{Z_{eff}/F}$) is $h_M^\pm(x_m) = (-I_p \pm \sqrt{4Z_{eff}F})$, $\|h_M\| = |h_M^+ h_M^-|^{1/2} = \delta_z \equiv \overline{h_B}$. At $F = F_a$, we have $\delta_z = 0$ ($d_B = \overline{h_B} = 0$), the barrier disappears and the direct or the barrier-suppression ionization starts.

In the (low-frequency) attosecond experiments, the laser field is comparable in strength to the electric field of the atom. Usually intensities of $\sim 10^{14} \text{ W cm}^{-2}$ are used. A key quantity is the Keldysh parameter [11],

$$\gamma_K = \frac{\sqrt{2I_p}}{F} \omega_0 = \tau_K \omega_0, \quad (2)$$

where ω_0 is the central circular frequency of the laser pulse and τ_K denotes the Keldysh time. In eq 2 and hereafter, we adopt

* Electronic mail: kullie@uni-kassel.de

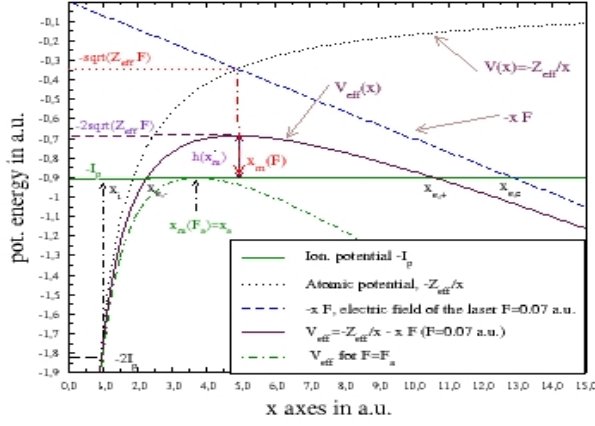


FIG. 1. (Color online) Graphic display of the potential and the effective potential curves, the two inner and outer points $x_{e,\pm} = (I_p \pm \delta_z)/2F$, the barrier width $d_B = x_{e,+} - x_{e,-} = \delta_z/F$. $\delta_z = \sqrt{I_p^2 - 4Z_{eff}F}$, I_p is the ionization potential, Z_{eff} is the effective nuclear charge and F is the electric field strength of the laser pulse at maximum. $x_{e,c} = I_p/F \equiv d_C$ the “classical exit” point and $x_m(F) = \sqrt{Z_{eff}/F}$ the position at the maximum of the barrier height $h_B(x)$, $h_M = -I_p + \sqrt{4Z_{eff}F}$. $x_a = x_m(F = F_a)$, F_a is the atomic field strength, see text. The plot is for He-atom in the single-active-approximation model with $Z_{eff} = 1.6875$ and $I_p = 0.90357 au$. For systems with different Z_{eff} , I_p the overall picture stays the same.

the atomic units (au), where the electron’s mass and charge and the Planck constant are set to unity, $\hbar = m = e = 1$. According to Keldysh or strong-field approximation (SFA), for values $\gamma_K > 1$ the dominant process is the multiphoton ionization (MPI). On the opposite side, i.e. for $\gamma_K < 1$ (actually $\gamma_K \ll 1$), the ionization (or field-ionization) happens by a tunneling process, which occurs for $F < F_a$. This result is highly refined later and is known under the Keldysh-Faisal-Reiss (KFR) theory [12, 13], where the two regimes of multiphoton and tunneling are more or less not strictly defined by γ_K [14–16]. Unfortunately, as we will see in the present work, the celebrated separation between tunneling ($\gamma_K \ll 1$) and multiphoton regime by Keldysh parameter, loses its meaning when a nonadiabatic ionization (nonadiabatic field calibration [17]) is considered. Obviously, the process is now described mainly by a multiphoton mechanism, and as we will see, a tunneling contribution is involved at the top of the barrier. Again similar to the adiabatic case, we find that the ionization time is a delay time with respect to the quantum limit of the ionization time at atomic field strength F_a .

In the experiment with He-atom [1, 17], an elliptically polarized laser pulse is used with $\omega_0 = 0.062 au$ ($\lambda \approx 735 nm$) and with ellipticity $\epsilon = 0.87$. The electric field strength is varied in the range $F \approx 0.02 - 0.10$ in nonadiabatic ($F \approx 0.04 - 0.11$ in adiabatic) calibration and for He atom $I_p = 0.90357 au$. In the attosecond angular streaking experiment, one uses a close-to-circular polarized laser pulse, where the direction of laser

field ensures a unique relationship between the time at which the electron exits the potential barrier and the direction of its momentum (offset angle) after the laser pulse [1–3, 17].

The main result of our tunneling model is the following T-time formulas [4],

$$\begin{aligned} \tau_{T,d} &= \frac{1}{2(I_p - \delta_z)}, \quad \tau_{T,i} = \frac{1}{2(I_p + \delta_z)}, \\ \tau_{tot} &= \tau_{T,i} + \tau_{T,d} = \frac{I_p}{4Z_{eff}F} \end{aligned} \quad (3)$$

The physical reasoning of the relations is the following: the presence of a barrier causes a delaying time $\tau_{T,d}$, which is a time delay with respect to the ionization at atomic field strength F_a , when the barrier disappears $\delta_z = 0$, $d_B = 0$. It is the time duration to pass the barrier region (between $x_{e,-}$, $x_{e,+}$) and escapes at the exit point $x_{e,+}$ to the continuum [4]. Whereas $\tau_{T,i}$ is the time needed to reach the entrance point $x_{e,-}$ from the initial point x_i , compare fig 1.

The two steps of the model coincide at the limit $F \rightarrow F_a$ ($\delta_z \rightarrow 0$), and the total time is $\tau_{tot} = \frac{1}{I_p}$, or $\tau_{T,d} = \tau_{T,i} = \frac{1}{2I_p}$ at the atomic field strength F_a . For $F > F_a$, the barrier-suppression ionization sets up [18, 19]. At the opposite side of the limit, we have $F \rightarrow 0$, $\delta_z \rightarrow I_p$ and $\tau_{T,d} \rightarrow \infty$. Hence, nothing happens and the electron remains in its ground state undisturbed, which shows that our model is consistent. For details, see [4, 20–22].

B. Tunneling and Ionization time delay

In this section, we show that the delay time in our tunneling model (eq 3) can be understood in a different way, which accounts to the nonadiabatic effects. Eq 3 can be decomposed is a twofold time delay with respect to ionization at F_a . It explains the tunneling time in a more advanced picture. We can rewrite the tunneling time τ_d in eq 3 as the following

$$\begin{aligned} \tau_{T,d} &= \frac{1}{2(I_p - \delta_z)} = \frac{1}{2} \frac{I_p}{4Z_{eff}F} \left(1 + \frac{\delta_z}{I_p} \right) \\ &= \frac{1}{2I_p} \left[\frac{F_a}{F} \left(1 + \frac{\delta_z}{I_p} \right) \right] = \tau_a \chi(F) \\ &= \frac{1}{2I_p} \frac{F_a}{F} + \frac{1}{2I_p} \frac{F_a}{F} \frac{\delta_z}{I_p} = \tau_a \zeta_F + \tau_a \Lambda_F \\ &= \tau_{dion}(F) + \tau_{delt} \end{aligned} \quad (4)$$

The second line in eq 4 immediately shows that our tunneling time can be easily interpreted as a delay time with respect to ionization at atomic field strength $\tau_a = \tau_d(F_a) = 1/(2I_p)$, which is real and quantum mechanically does not vanish, where $\chi(F)$ is an enhancement factor for field strength $F < F_a$. In the third line, we see that both terms are time delays and real. The second term, τ_{delt} , is real because $\delta_z > 0$ is a real

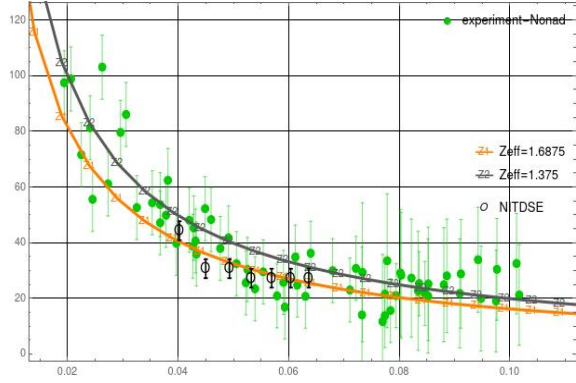


FIG. 2. (Color online) Graphic display, ionization time versus field strength. Our ionization time τ_{dion} as given in eq 6 for two $Z_{eff} = 1.6875(Z_1), 1.375(Z_2)$, with the experimental data of Hofmann in the new calibration of the field strength [17]. NITDSE (open circle) from [24], see text

quantity [4]. The first term in eq 4 is an ionization time delay, solely because F is smaller than the atomic field strength F_a , whereas the second term is a delay time due to the barrier itself, which is the actual T-time as discussed in details in the recent work [22].

We note that the separation in a twofold time delay in eq 4, represents a unified T-time picture in accordance with the unified T-time picture found by Winful (UTP) [23] for the quantum tunneling of a wave packet or a flux of particles scattering on a potential barrier. Winful showed that the group time-delay or the Wigner time-delay can be written in the form

$$\tau_g = \tau_{si} + \tau_{dwell}, \quad (5)$$

where τ_{dwell} is the dwell time which corresponds to our τ_{delt} , and τ_{si} is according to Winful a self-interference term, which corresponds to our τ_{ion} . For details, we kindly refer the reader to our recent work [22].

It is now clear, ionization and tunneling can be categorized by two time delays with respect to the atomic field strength, where the entire process is triggered by the field disruption of the laser pulse. That is completely different to the well known separation by the Keldysh parameter in strong field theory, where one commonly uses γ_K to divide the process in two regimes, the multiphoton $\gamma_K > 1$ and the tunneling $\gamma_K \ll 1$ regime. The intermediate regime is assumed to incorporate a coexistence of tunneling and multiphoton ionization, and even the tunneling regime is usually extended to cover $\gamma_K \sim 1$ [1]. In fact, the separation is not strict and is usually applied vaguely.

Fortunately, we are able to account for the nonadiabatic effects, where we mainly mean photons (multiphoton) absorption, i.e. other effects are small or negligible as discussed by

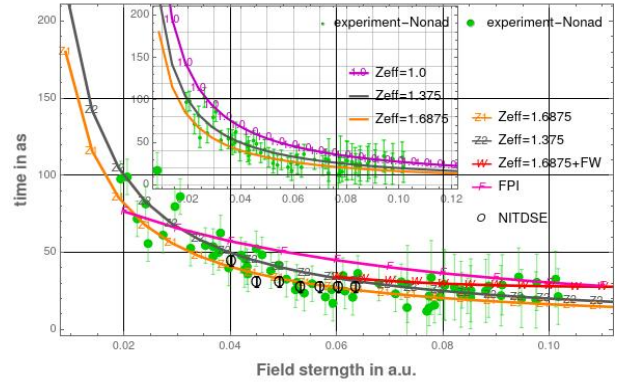


FIG. 3. (Color online) Graphic display, ionization time versus field strength. Plots as given in fig 2 but with an additional curve (W, red curve) for $Z_{eff} = 1.6875$ with $I_p \rightarrow I_p + (\frac{F}{2\omega_0})^2$ (see [25] chap. 2, p.19), and the FPI result (F-curve) from [17]. An enlarged axes ranges to show that our ionization time τ_{dion} gives perfectly the trends of the experimental data (see discussion in the text). In the inset the curves for three Z_{eff} (from below) 1.6875, 1.375, 1.0.

Hofmann et al [17]. The number of the absorbed photons is determined by the barrier height (which depends on the field strength, see fig 1). We find that the second term in eq 4, i.e. the barrier (height) is overcome by multiphoton absorption, and that the nonadiabatic calibration is mainly just that, as we will see in the following. Such a process is usually incorporated in the intermediate regime, i.e. photons absorption while tunneling through the barrier, but no clear picture is given, see sec D. Nevertheless, the process is primarily a multiphoton ionization, which can be understood as the following

$$\begin{aligned} \tau_{dion}(F) &= \frac{1}{2I_p} \frac{F_a}{F} + \frac{1}{2I_p} \frac{F_a}{F} \overbrace{\left(\delta_z - n_F \omega_0 \right)}^{\approx 0} \\ &= \frac{1}{2I_p} \frac{F_a}{F} = \frac{1}{2I_p} \zeta_F = \tau_a \zeta_F \end{aligned} \quad (6)$$

The relation in eq 6 shows a very good agreement with the experimental data in the nonadiabatic calibration of Hofmann et al [17], as shown in fig 2, 3, where we plot $\tau_{dion}(F)$ together with the experimental data of Hofmann et al. In eq 6, ω_0 is the central frequency of the laser pulse, and n_F with $0 \leq n_F = \text{floor} \left(\frac{\delta_z}{\omega_0} \right) \leq n_{I_p} = \text{floor} \left(\frac{I_p}{\omega_0} \right)$, is the (minimum) number of photons required to (climb) overcome the barrier height at a field strength F , which is the barrier (energy) gap δ_z , as discussed in [20], compare fig 1. Note, in the perturbation regime where F is too small, we have $\delta_z \approx I_p$, $n_F = n_{I_p}$. Whereas for a strong field strength, n_p is reduced by a factor, which depends on the field strength $n_F = n_{I_p} \sqrt{1 - F/F_a} \leq n_{I_p}$. The function $\text{floor}(x)$ gives the round down of a real number x , where one usually uses $\text{floor}(x) + 1$ (e.g. $n_{I_p} + 1$) in the perturbation regime.

Note that in eq 6 the enhancement factor ζ_F is a relative dimensionless factor, and we can use the intensity instead of

the field strength, $\zeta_F = \zeta_I^{1/2} = \sqrt{I_a/I_L}$, where $I_a = F_a^2$ is the appearance intensity [9] and I_L the intensity of the laser pulse.

Looking to our result as shown in figs 2, 3, we find interesting features. The strong field interaction actually is dominated by the multiphoton ionization process, as far as nonadiabatic calibration is concerned, e.g. as done by Hofmann et al [17]. Therefore, the question now what or where is the difference between the weak and strong field interaction processes, since we mainly encounter a multiphoton ionization (process) in this experimental calibration of the strong field regime.

It seems that one of the main effects, if not the main effect, is shrinking or lowering down the gap to $\delta_z < I_p$, up to $\delta_z \approx 0$ at $F = F_a$, whereas for too small field strength ($F \rightarrow 0$) $\delta_z \approx I_p$. The delay time is determined by the enhancement factor ζ_F (or $\chi(F)$ for the adiabatic case), which becomes unity at $F = F_a$, at which the ionization time reaches its limit $\tau_{dion}(F_a) = \tau_a = 1/(2I_p)$. Nevertheless, as far as nonadiabatic calibration is concerned, the so called tunneling regime is incorporated in the multiphoton process. Because the error bars of the experiment are large (see fig 2, 3), it is difficult to verify that after photons absorption a tunneling occurs slightly below the barrier top, we discuss this issue in details in sec D. Indeed, one can better understand this point by eliminating the other nonadiabatic effects, e.g. due to laser pulse duration (envelope) and intensity fluctuations, which in our view is responsible for the spread of experimental points. Hofmann [26] noted that between recording one distribution to the next, the laser parameters, setup, temperature in the lab, might change and have a slight influence, in principle the data point should also have error bars for their F-axis-position.

It is worthwhile to mention that many authors use a different definition for the atomic field strength, e.g. $F_a^K = k^3 = (2I_p)^{3/2}$ [27, 28], which is related to the Keldysh parameter. It actually leads to the Keldysh time as we can see by the substitution $F_a \rightarrow F_a^K$ in eq 6

$$\frac{1}{2I_p} \frac{F_a^K}{F} = \frac{1}{2I_p} \frac{k^3}{F} = \frac{2I_p}{2I_p} \sqrt{2I_p} F = \frac{\sqrt{2I_p}}{F} = \tau_K$$

It is well known that Keldysh time is too large, a classical quantity and does not describe tunneling or (multiphoton) ionization time, for details see [20]. This, however, shows that our time delay of eq 6 is directly connected to the strong field theory, where ζ_F represents the correct parameter to determine the delay time while the atomic field strength is given by $F_a = \frac{I_p^2}{4Z_{eff}}$, regardless of the Keldysh parameter γ_K . Hence, the Keldysh parameter loses its significance in characterizing

different regimes in the nonadiabatic strong field approximation, or precisely in the nonadiabatic field calibration.

Since $\delta_z \approx n_F \omega_0$, $n_F = \text{floor}(\frac{\delta_z}{\omega_0})$, a tunneling mechanism happens rather near the threshold slightly below the top of the barrier as already mentioned, where $\frac{\delta_z}{\omega_0}$ is usually not an integer, and the absorption of n_F photons lets a fairly small energy gap $\frac{\delta E}{\omega_0} = (\frac{\delta_z}{\omega_0} - n_F) < 1$, which permits a tunneling mechanism, see further below sec D. However, the interaction process is more complicated, and as we have discussed in [21] a scattering mechanism and a nonlinear Compton scattering can be involved, where energy and momentum transfer to the tunneled or ionized electron are possible. They are related to the characteristic of the interaction of the electron with the intense laser field [29] by $\sim \left(\frac{F}{\omega_0}\right)^2$ and $\sim \alpha \left(\frac{F}{\omega_0}\right)^2$, respectively. $\alpha = 1/c$ (c the speed of light) is the fine structure constant, which is equal to the strength of the interaction of the photon with the electron.

In short, the number of the absorbed photons n_F is smaller than $n_{I_p} = \text{floor}(\frac{I_p}{\omega_0})$. Only in the limit $F \rightarrow 0$, the gap becomes close to the ionization energy $\lim_{F \rightarrow 0} \delta_z = I_p$ and $n_F = n_{I_p}$. The case $I_p/\omega_0 \gg 1$, $F \ll F_a$ is commonly known as a perturbation (multiphoton) regime through an absorption of n_{I_p} photons (usually in the literature $n_{I_p} + 1$ is used [25]). We think that eq 6 is also valid in this regime as we can see from fig 3.

This way we are able to reach a very good agreement with the revised experimental result of the nonadiabatic calibration of the field strength of Hofmann et al [17], as was the case in the adiabatic calibration of Landsman et al [1]. We kindly refer the reader to compare fig 2 in the present work with fig 4 in [4]. In the figs 2, 3 the lower curve (orange) for an effective nuclear charge of Clementi [30] $Z_{eff} = 1.6875$, and the upper (gray) curve for $Z_{eff} = 1.375$. As seen, the difference between the two curves is smaller than the error bars, thus, the value of Z_{eff} is not crucial. See further below sec C. We also show in the figures the Feynman path integral (FPI) from the same work of Hofmann et al is shown, in figs 2, 3 the (purple) F-curve. In addition, we plotted data from numerical integration of time-dependent Schrödinger Equation (NITDSE) presented by Ivanov et al [24] (empty circles with small error bars), which shows an excellent agreement with our result. Looking back to this earlier result we find that the NITDSE was compared to experimental data of Boge et al [31] using non-adiabatic calibration. The data of Boge et al [31] (see further below fig 8) differs slightly (a bit higher) from the data of Hofmann et al [17], so that the NITDSE result of Ivanov et al was not close to the experimental data of Boge et al as it is the case in fig 2, 3, see discussion in [21]. It is possible that Hofmann et al

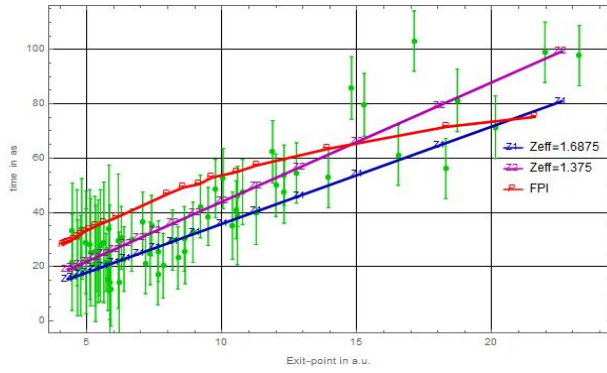


FIG. 4. (Color online) Ionization time versus exit point $x_{exit} = I_p/(2F)$ for $Z_{eff} = 1.6875$ (below), $Z_{eff} = 1.375$ (above). Experimental data as in figs 2, 3. The FPI result (F-curve) from [17] is included but by using $x_{exit} = I_p/(2F)$ (compare with fig 13 of [17])

have benefited from the NITDSE result of Ivanov et al by the nonadiabatic calibration of the field strength, hence, the good agreement with NITDSE, as seen in figs 2, 3. However, the good agreement between these results, our result, the NITDSE and the recent experimental data of Hofmann et al shows that the issue is now pretty well resolved.

Using $Z_{eff} = 1.0$ is unrealistic specially for field strengths in the region near F_a . The curve with $Z_{eff} = 1.0$ is plotted in fig 3 (inset, upper curve). It matches some of the experimental points for $F < 0.03$. It is expected to better fit an experimental result with small field strengths $F < 0.02$, where no experimental points are presented. It is also very close to the FPI for $F \geq 0.05$ (and the Larmer clock, data not shown, see [17]). This is not expected, but possibly because the value $Z_{eff} = 1.0$ is used in the FPI calculation. Nevertheless, the FPI result does not fit well to the experimental result. In contrast to the flat behavior for larger field strengths (especially close to F_a), for smaller field strengths $F \leq 0.02$ the curves get very steep with a large slope, see fig 3. Nonetheless, we think that the (ionization) time delay given in eq 6 is valid for small field strengths, as we mentioned above. In fact, the main behavior of the time delay is determined by the $\sim \frac{1}{F}$ dependence, which is similar to the classical behavior or the Keldysh time [20]. In fig 3, we also plotted an additional curve (red w-curve) of the time delay (with $Z_{eff} = 1.6875$) for field strengths $F \geq 0.05$, by including the shift of the continuum given by $F^2/(2\omega_0)^2$ [25], which it is negligible for $F < 0.05$. This makes our curves flat approaching a horizontal line. In principle this sets a lower limit for the Ionization time, and the delay time does not fall below this limit, unless there is another effect to cause a deviation (but to higher time delay) such as in the above-threshold ionization (ATI) by absorption additional photons, i.e. larger than n_F , which we address in future work [32].

We note that our model, by including the nonadiabatic effects, is related to the original one (adiabatic), as seen from eqs 4, 6. This is important because our forms, the adiabatic and nonadiabatic, together offer now a detailed picture of the interaction with the laser pulse and an unified picture for the tunneling and multiphoton regimes in accordance with Winful UTP, as we already mentioned. Most of the works in the literature still puzzle about a separation into two regimes (tunneling and multiphoton), usually defined by Keldysh parameter γ_K of eq 2.

C. The exit point and the dynamics of the process

It is usual in the strong field or ultra fast science to use the so called classical exit point $x_C = I_p/F$, see fig 1, to characterize spatially the point at which the tunneled or ionized electron escapes the potential barrier or the atomic potential, for details see [20]. Depending on the concept used to characterize the tunneling process, it becomes a free particle at the exit point (real tunneling time picture [4]), or it becomes subject to the tail of the potential (imaginary tunneling time picture [5]). A quick look to fig 1 shows immediately that $x_C = I_p/F \equiv d_C$ is inaccurate and even wrong. However, Hofmann et al has used x_C in their recent work [17]. For the adiabatic tunneling, it was shown in [33] that the correct exit point is $x_{e,+}$ (compare fig 1) and the use of x_C (or d_C) leads to an erroneous conclusion. In the nonadiabatic case (the present work), the exit point $x_{e,+}$ is not suitable because the barrier height is now overcome by photons absorption. We expect a major effect on the exit point $x_{e,+}$. Recalling what we did in eq 6 we find:

$$x_{e,+} = x_{e,-} = x_E = \frac{I_p \pm \overbrace{(\delta_z - n_F \omega_0)}^{\approx 0}}{2F} = \frac{I_p}{2F} = x_C/2 \quad (7)$$

The initial point $x_i = Z_{eff}/(2I_p) \sim 1a.u.$ is small and can be fairly neglected. We note that with eq 7 the barrier width vanishes $d_B = x_{e,+} - x_{e,-} = 0$, whereas the traversed distance in this case is $d_h = x_{exit} - x_i \approx x_E$. The process of photons absorption is usually depicted as a vertical process [34], i.e. the electron climbs the potential energy vertically. Clearly at the same time, it moves and escapes the Coulomb potential of the atom at x_E and becomes a free particle. In fig 4, we plot the ionization time as a function of the exit point $x_E = \frac{I_p}{2F}$. Nevertheless, because $x_E = x_C/2$ the overall picture is similar to the case of the adiabatic calibration, see fig 2 of [33]. We see a linear scaling of the time delay with the exit point, clearly because the same $\sim \frac{1}{F}$ dependence of eqs 6, 7.

However, we can characterize the exit point in a different way. As seen in fig 1, the maximum of barrier height is located

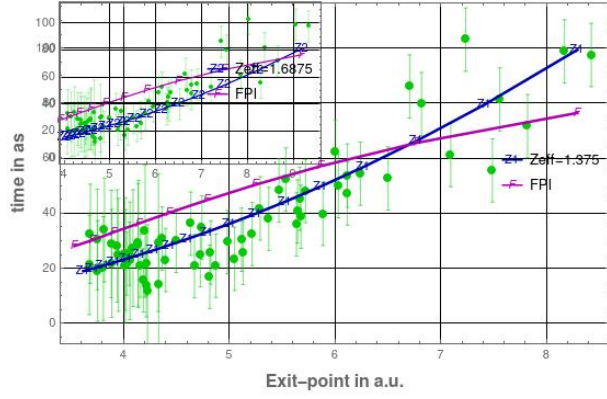


FIG. 5. (Color online) Graphic display data of Hofmann in the new calibration of the field strength. Ionization time versus exit point $x_m = \sqrt{Z_{eff}/F}$, with $Z_{eff} = 1.375$ and $Z_{eff} = 1.6875$ (Inset). F-curves: FPI-curves

at $x_m = \sqrt{\frac{Z_{eff}}{F}}$ and we expect that the ionized electron will climb vertically the barrier (actually the effective potential) and escape at x_m , the location of the maximum of the effective potential curve. In fig 5, we plot the ionization time versus the exit point $x_m = \sqrt{\frac{Z_{eff}}{F}}$ for the two $Z_{eff} = 1.375, 1.6875$. Unlike x_E , the exit point x_m , and hence, the curves in fig 5 depend on Z_{eff} . The difference to fig 4 is not remarkable, although x_m is noticeably smaller. Unlike the former case in fig 4, the curves in fig 5 are not straight lines. However, from the comparison of the two figures 4, 5 it is difficult to judge which one exactly determines the exit point. In fact, from the good agreement of eq 6 with the experimental data (as seen in fig 2) for Z_{eff} values larger than 1.0, i.e. $Z_{eff} = 1.6875, 1.375$, we think that the traversed distance by the ionized electron should not be too large (not too far from the nucleus.) Since x_m is significantly smaller than x_E (eq 7), most likely that the actual exit point is rather close to x_m . See further in below sec D. x_m is more reliable since the electron move to the maximum of the barrier height while it absorbs n_F photon, where the (multiphoton) ionization is dominated by the vertical channel [34]. That is unlike the adiabatic case, where no photon absorption involved in the tunneling process. In the later case the horizontal channel dominates the process of tunneling (field-)ionization [34]. Finally, the so called classical exit point x_C is by no mean a correct choice (compare fig 1), see also [33] for the adiabatic case. Indeed, it is easy to see from the barrier width

$$d_B = \frac{\delta z}{F} = \frac{I_p}{F} \sqrt{1 - 4Z_{eff}/I_p^2} = x_C \sqrt{1 - \zeta(F)}$$

that x_C is modified by a factor, which become unity at small field strength $\lim_{F \rightarrow 0} \sqrt{1 - \zeta(F)} \rightarrow 1$. Hence, the so called classical barrier width is justified only for $F \ll F_a$. In conclusion, we think that the correct traveled distance by the

ionized electron is most likely $x_m - x_i \approx x_m$, where x_i the initial point is small $\sim 1a.u$ and mostly negligible.

D. The intermediate regime

In our model we have treated so far two cases, the non-adiabatic field scaling in the present work and the adiabatic field scaling case in [4]. In both cases we found a good agreement with the experimental result. The nonadiabatic case of eq 6 is shown in figs 2, 3 with the experimental data of Hofmann et al [17]. The adiabatic case of eq 3 was shown in [4] with the experimental data of Landsman et al [1]. The field scaling of Hofmann et al affects a shift to a lower intensity. It causes a shift of the time delay to a smaller time value for the same field strength. This confirms our tunneling model as seen in eq 4, since the second term due to the barrier itself vanishes $\tau_{delt} = 0$, when the barrier is overcome by multiphoton absorption. A feature of the experimental data (both adiabatic and nonadiabatic), as seen in fig 7, is the spread of the points. This can be due to various reasons, such as pulse length or carrier envelope phase. However, as we will see below this can also be caused by intensity fluctuations.

It is now obvious that the above mentioned cases are two limits. This immediately raises the question about the intermediate regime, in which the number of absorbed photons is smaller than n_F given in eq 6. In general, we can set $0 \leq n_p \leq n_F$ with $n_p = 0, 1, 2 \dots n_F$, and we obtain

$$\begin{aligned} \tau_{tion}(F) &= \frac{1}{2I_p} \frac{F_a}{F} + \frac{1}{2I_p} \frac{F_a}{F} \frac{(\delta z - n_p \omega_0)}{I_p} \\ &= \frac{1}{2I_p} \left[\frac{F_a}{F} \left(1 + \frac{(\delta z - n_p \omega_0)}{I_p} \right) \right] \\ &= \tau_a \eta(F, \omega_0, n_p) \end{aligned} \quad (8)$$

We summarize the delay time as the following

$$\tau = \begin{cases} \tau_{T,d} = \tau_a \chi(F) & n_p = 0 \text{ adiabatic} \\ \tau_{dion} = \tau_a \zeta(F) & n_p = n_F \text{ non-adiabatic} \\ \tau_{tion} = \tau_a \eta(F, \omega_0, n_p) & 0 < n_p < n_F \text{ immediate} \end{cases}$$

With the help of eq 8, we can treat the intermediate regime which is usually referred to as photon absorption while tunneling. It is described qualitatively by Ivanov et al [34]. Recently, Klaiber et al [35] explained it with the help of the scattering theory as a transition region, in two steps. First the atom is polarized by virtual multiphoton absorption (the electron gains energy), followed by the subsequent tunneling out from the weakly bound virtual states (off-shell) of the polarized atom. In the work of Klaiber et al [35] the tunneling from the ground

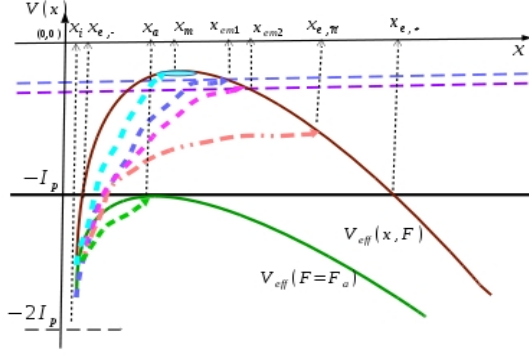


FIG. 6. Illustration of the the intermediate regime, eqs 8-10. The (orange) dashed dotted curve illustrates the view of Klaiber et al [28], which is usually called the nonadiabatic or immediate tunneling regime [34], see text eqs 7-10. For the different notation see fig 1.

state (no virtual photon absorption) corresponds to the adiabatic case. Furthermore, the opposite limit, called the direct multiphoton ionization, corresponds to our nonadiabatic case, as discussed in eq 6.

However, in our nonadiabatic picture the off-shells of the atoms (near the top of the barrier) are accessed by multiphoton absorption. In fig 6, we show an illustrative picture of two intermediate cases near the top of the barrier, in which the multiphoton absorption is followed by a tunneling from two immediate states near the top. These are the tow curves blue and purple with the exit points x_{em1}, x_{em2} , respectively. Whereas the highest curve (light blue) is the one without a tunneling contribution, $n_p = n_F$, with exit point x_m . Also is shown the limit case $F = F_a, \delta_z = 0$ with the exit point $x_m(F_a) = x_a$. In the later case, the atom is highly polarized that the barrier disappears, compare fig 1. The time to reach the entrance point x_a (which coincide with the exit point) is the quantum limit τ_a , see eq 6. This picture agrees well with the scattering and the collisional rearrangement process in the ion-atomic collision [35, 36]. It was discussed by Kullie in [6], where a nonlinear Compton type scattering with laser pulse is proposed, following the experimental investigation of Meyerhofer et al [29] and earlier theoretical work of Eberly et al [37]. It is a collective scattering with the laser wave packet with (high) photon density, i.e. strong field, where the electron recoil or the electric density is strongly polarized due to the strong electric field of the laser, similar to the ion-atom collision, as discussed by Klaiber et al [35]. Note, the effect cased by an electric field or a charge density is the same. Actually, according to Einstein, Wheeler and Feynman electric charge and field are the same and not independent entities [38]. We conclude that the collective scattering by the laser pulse, causes a polarization of the electronic density proportional to the electric field, which suppresses the barrier that

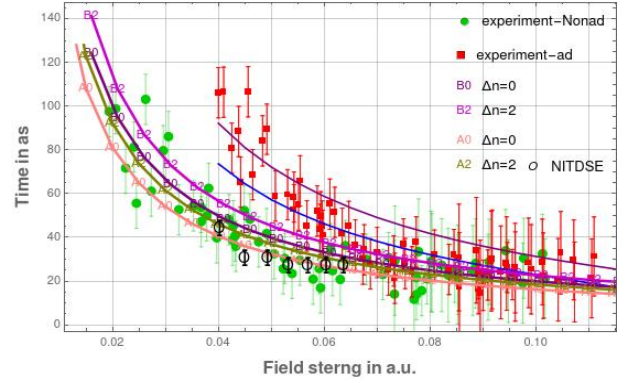


FIG. 7. (Color online) The figure show delay times τ_{tion} given in eq 11 for $Z_{eff} = 1.6875$ and $\Delta n = 0, 2$ (lower two A-curves). And $Z_{eff} = 1.375$ and $\Delta n = 0, 2$ (upper two B-curves). The experimental data (red, rectangles) with the adiabatic [1] and (green, circles) with non-adiabatic [17] field scaling, respectively. The two curves over the adiabatic experimental data (red, rectangle) are the T-time $\tau_{T,d}$ of eq 3 for $Z_{eff} = 1.6875$ (below), $Z_{eff} = 1.375$ (above). NITDSE (circle) as in fig 2 [24], see text.

only a number of photons $n_F < n_I$ is required for the multiphoton process in strong field. The delay time is then given by eq 6 and the limit is reached by $F = F_a$, where $d_B = 0, n_F = 0$ and $\tau_{dion} = \tau_a = 1/(2I_p)$. Whereas by a smaller number of photon $n_p < n_F, \Delta n = n_F - n_p > 0$ a tunneling mechanism accompanies the process from virtual states (compare fig 6), which rises the delay time above the self-interacting part as given in eq 8 for $0 < n_p < n_F$, see also further below eq 11.

In fig 7, we plot eq 8 for $Z_{eff} = 1.6875$ (lower two curves), and $Z_{eff} = 1.375$ (higher two curves), where for better visibility only the curves correspond to $n_p = n_F$ and, $n_p = n_F - 2$ are potted (referred to as $\Delta n = 0, 2$, respectively). According to this result we think that the spread of the experimental points corresponds to the absorption of $n_p \lesssim n_F$ photons as given in eq 8, though it is difficult to ensure such a conclusion, owing to the fact that the error bars are larger than the separation between successive curves ($n_p, n_p + 1$), see eq 8. We come back to this point later.

Concerning the exit point, in the general case of eq 8, it lies between x_m in the nonadiabatic case (no tunneling contribution) or the vertical channel and $x_{e,+}$ in the adiabatic case (only a tunneling mechanism) or the horizontal channel, compare fig 6. An approximate value can be obtained by the same procedure applied in eq 8,

$$x_{n,\pm} = \frac{(I_p \pm \delta_z - n_p \omega_0)}{2F}$$

It shifts the exit point from x_m for $n_p = n_F$ towards $x_{e,m1}, x_{e,m2}, \dots$ for $n_p < n_F, \Delta n = 1, 2, \dots$ and reaches in the adiabatic case $x_{e,+}$ for $n_p = 0$, see fig6. The barrier width

changes in the same way, which leads to

$$\begin{aligned} d_B^n &= \frac{(I_p + \delta_z - n_p \omega_0)}{2F} - \frac{(I_p - \delta_z + n_p \omega_0)}{2F} \\ &= \frac{(\delta_z - n_p \omega_0)}{F} = \frac{\omega_0}{F} (n_F - n_p) = \frac{\omega_0 \Delta n}{F} \end{aligned} \quad (9)$$

For $F = F_a$, we have $d_B = 0, \delta_z = 0, x_{n,\pm} = 2Z_{eff}/I_p = \sqrt{Z_{eff}/F_a} = x_m(F_a) = x_a$. With eq 9 we can approximate the exit point (compare fig 6),

$$x_{e,m} \approx x_m + \frac{d_B^n}{2} = \sqrt{\frac{Z_{eff}}{F}} + \frac{\omega_0 \Delta n}{2F} \quad (10)$$

Note, for $n_p = n_F; \Delta n = 0$, we have $d_B^n = 0$ and $x_{em0} = x_m$. In this case, the ionization happens along the vertical channel and there is no tunneling contribution, as discussed before. Therefore, the second term in eq 10 indicates a tunneling contribution. The interesting case is the tunneling near the top of the barrier, that is when $\Delta n \sim 1, 2$ is small enough that the tunneling probability is large (compare fig 6). In our view, the spread of the experimental points can be tracked back to this issue, as already mentioned. This can be further explained as the following. We see from eq 9 that the difference in the number of absorbed photon changes the exit point from x_m for $\Delta n = 0$ to x_{em1}, x_{em2}, \dots for $\Delta n \sim 1, 2, \dots$. It also changes the ionization time from the nonadiabatic case τ_{dion} (eq 6) when $n_p = n_F, \Delta n = 0$ towards the adiabatic case $\tau_{T,d}$ (eq 3) for $n_p = 0, \Delta n = n_F$. Indeed, by rewriting eq 8 we obtain

$$\begin{aligned} \tau_{t ion}(F) &= \frac{1}{2I_p} \frac{F_a}{F} \left(1 + \frac{(\delta_z - n_p \omega_0)}{I_p} \right) \\ &= \frac{1}{2I_p} \frac{F_a}{F} \left(1 + \frac{(n_F \omega_0 - n_p \omega_0)}{n_I \omega_0} \right) \\ &= \tau_a \frac{F_a}{F} \left(1 + \frac{\Delta n}{n_I} \right) \end{aligned} \quad (11)$$

Eq 11 is important, since it is valid for the intermediate tunneling, but is independent of the laser frequency ω_0 . One notices that Δn is the deviation from n_F . Hence, for $\Delta n = 0$ we have the self-interacting term as discussed in eq 5 [22]. It sets a lower limit to the delay time of the multiphoton ionization process or the vertical channel, as given in eq 6. The second term appears when $n_p < n_F, \Delta n > 0$, which is smaller than the first one and indicates a tunneling part, which increases the time delay. For small values $\Delta n \sim 1, 2$, the second term rises the delay time by a small amount. This can be seen in fig 7 for $\Delta n = 0, 2$ and $Z_{eff} = 1.6875, 1.375$, with the experimental data of Hofmann and Landsman (adiabatic case, see [4]). As we see in fig 7, for $\Delta n > 0$ the delay time increases from τ_{dion} toward the adiabatic limit $\tau_{T,d}$, the latter is the tunneling time and occurs when $n_p = 0, \Delta n = n_F$. For small Δn , the curves slightly shift above the curve of τ_{dion} , which is consistent with the spread of the experimental values. A

reason for the spread of the experimental could be intensity fluctuations of the laser pulse, which leads to the absorption of a smaller number of photons $n_p \lesssim n_F \Rightarrow \Delta n > 0$, following by a tunneling near the top of the barrier, compare fig 6.

This explanation is supported by the work of Serebryanikov et al [39]. With a modified SFA and for Hydrogen atom in high field intensities, they showed that tunneling ionization from excited states (e.g. intermediate tunneling) dominates over the tunneling of ground-state electrons, as we have discussed above with regard to the work of Klaiber et al [35]. Actually, even by only a vertical channel according to eq 6 by the absorption of $n_F = \text{floor}(\delta_z/\omega_0)$ photons, a tunneling mechanism is possible in a relatively narrow window $0 < \varepsilon = (\delta_z - n_F \omega_0) < 1\omega_0$ at the top of the barrier, the thin ellipse at the top in fig 6. Note, for relatively large ω_0 the tunneling contribution should be clearly observable in the experiment. We think this is important to indicate and specify the tunneling contribution in strong field science and the attoclock.

In conclusion, there is a small contribution of tunneling (horizontal channel). For small $\Delta n = 1, 2$ (eq 11) the amount of this contribution is smaller than the error bars in the data of Hofmann et al [17]. Hence, a refinement on the experimental side should be able to explain this issue.

We further notice that Klaiber et al in [28] presented a result, by considering the experimental data of Boge et al [31]. The Keldysh parameter $\gamma_K \sim 0.3 - 5.9$ is in the immediate region, which is the same range as in the nonadiabatic field scaling of Hofmann et al [17]. They argued that the electron absorbs an effective number of photon \tilde{n} followed by a static tunneling at higher energy $E = -I_p + \tilde{n} \omega_0$ what they called a rule of thumb for the region $\gamma_K \lesssim 1$. However, no specification of \tilde{n} is given, but I think it should be compared with our n_p in eq 8 (see also eq 11). This rule supposed to shift the exit point from the the quasi-static exit point $x_{e,qs} = I_p/F = x_{e,C}$ (fig 1) to the exit point $x_e = x_{e,qs} - \delta x$, although as we noted before $x_{e,C}$ is not correct (compare fig 1). The view of Klaiber et al is shown in fig 6 by orange dashed line with the exit point $x_{e,\tilde{n}}$ (compare with fig 1 of [28]). According to Klaiber et al [28], in the nonadiabatic regime the electron gains energy in the course of the under-the-barrier motion, and the nonadiabatic corrections rises the energy level and the tunnel exit shifts closer to the atomic core. They compared the emission angle of the most probable trajectory with the experimental data of Boge et al [31], for He atom. The nonadiabatic time delay claimed by Klaiber et al in [28] is due to two factors: the ionization barrier is changing during the tunneling formation in the nonadiabatic case, and the bound state is not localized

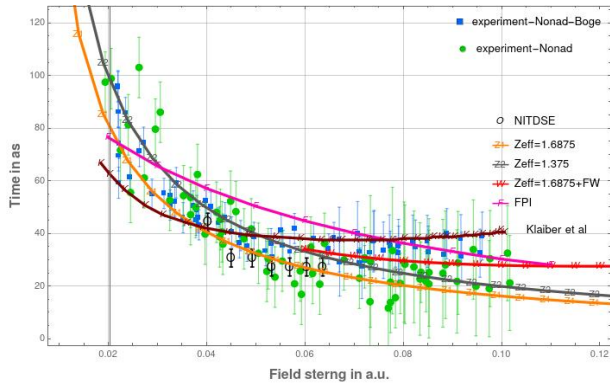


FIG. 8. (Color online) The figure show delay times τ_{tion} given in eq 6 for $Z_{eff} = 1.6875$ and $Z_{eff} = 1.375$. As in figs 2, 3 the experimental data of Hofmann [17] (green circles) and NITDSE of (open black circles) [24] are shown, but we included the nonadiabatic experimental data (blue rectangles) of Boge et al [31] and the result of Klaiber et al [28] (K, dark curve), see text.

in the case of a Coulombic atomic potential. In fig 8 we show again our result and include the experimental data of Boge et al and the the result of Klaiber et al (see fig 2 of [28]). We have to mention that both experimental results are from the same group at ETH Zurich, where the recent experimental result of Hofmann et al [17] is supposed to be superior. To compare with our result the data of Boge et al and Klaiber et al have been converted from angle to time. As we see in fig 8, the result of Klaiber et al fits somehow the experimental result, but despite an intricate procedure which combines analytical and numerical parts (see [28] and the supplementary information) the correct trend is not satisfactory. The later is determined by the $\sim \frac{1}{F}$ dependency of the delay time.

Although Klaiber et al [28] interpreting the time delay in a different way [28], we think that the agreement with our result implies an important point. Namely, it gives a clear hint that the emission angle or equivalently the time delay is mainly due to the barrier region (or under-the-barrier motion [28]) and not due to the tail of the potential as claimed by the imaginary tunneling time picture, as discussed in our previous works (real tunneling time picture) [4, 6, 20–22]. The nonadiabatic case is mainly explained by the multiphoton ionization, as we have discussed in this work. Similarly the intermediate regime, as given in eq 11 and fig 7, 6. The comparison of the nonadiabatic and adiabatic cases in fig 7, shows immediately that the delay time in the later case increases due the effect of the barrier itself, the second term τ_{delt} in eq 4. It is absent by field scaling of Hofmann et al [17] that affects a shift toward smaller field strength (larger self-interference contribution). Equivalently, for the same F a greater delay time in the adiabatic case comes out compared to the nonadiabatic case, due to the second term τ_{delt} . Actually, it maps ΔF to Δt , which confirms the real

tunneling picture. For $F \rightarrow 0$ we reach a maximal delay time Δt , that is $\lim_{F \rightarrow 0} \tau = \infty$, as we have seen in eq 3 $\lim_{F \rightarrow 0} \delta_z = I_p, \tau_d \rightarrow \infty$. The physical relevance of our conclusion concerns the theory of tunneling.

Finally, many experimental points (compare fig 7) are below the limit of τ_{dion} ($\Delta n = 0$), it can not be explained this way. Since the use of SAE or the Z_{eff} is not crucial as discussed in [17], it is difficult to understand this behavior. Multielectron effects are also small, they could be important for small barrier width perhaps $F > 0.05$. But hardly explain this behavior for larger barrier width, where one has to use $Z_{eff} \sim 1.375$. One tends to argue that the spread of the experimental points should be improved with a better measurement procedure.

In short, with our model, we can explain the attoclock result. We find a very good agreement with experimental finding in the adiabatic [1] and non-adiabatic scaling [17]. We give a clear picture for an intermediate tunneling regime qualitatively and quantitatively. We think that eqs 6, 8, 11 are of general importance for the quantum optics, and not only for the strong field regime.

Conclusion In this work we have showed that our tunneling model is capable to tackle the nonadiabaticity and again (as before the adiabatic case [4]) we have reached a very good agreement with the experimental data in the non-adiabatic calibration of the attoclock of Hofmann et al [17]. Interestingly, our model offers a clear picture for the multiphoton process versus tunneling process. Particularly, in the nonadiabatic case, the barrier itself is overcome by photons absorption (the main nonadiabatic effect) and the time delay is now an ionization time delay with respect to the ionization at atomic field strength, where the barrier suppression ionization sets up. Further, we discussed the intermediate regime specially near the top of the barrier, where the tunneling probability is large. The delay time then comprises two parts, the self-interacting (multiphoton) part and a tunneling contribution. This way, we have resolved the controversial, not strict and vague separation (by Keldysh parameter γ_K of eq 2) of the strong field ionization into two regimes, the multiphoton and the tunneling regimes. Even if one persists with the two distinct interpretations the attoclock, adiabatic and nonadiabatic, in both cases the time of tunneling or (multiphoton) ionization is a (real) delay time with respect to the ionization at atomic field strength. If we consider the experimental data of Hofmann [17] to be the ultimate correct calibration, then the agreement presented in this work shows that strong field interaction is primarily driven by multiphoton ionization. A tunneling contribution is possible especially near the top of

the barrier and can be associated with an intermediate regime or intermediate tunneling. The attoclock receives a new boost and the subtlety of the experimental investigations is more demanding than ever before. The investigation of the tunneling or ionization using static field could be also an option in this direction, especially to resolve some of the questions regarding the tunneling process. The tunneling versus multiphoton ion-

ization in strong field, attosecond and ultrafast science have become more challenging than ever.

Acknowledgments I would like to thank C. Hofmann for sending the experimental data, and FPI values presenting in the figures. I would like to thank Prof. Martin Garcia from the Theoretical Physics of the Institute of Physics at the University of Kassel for his kind support.

-
- [1] A. S. Landsman, M. Weger, J. Maurer, R. Boge, A. Ludwig, S. Heuser, C. Cirelli, L. Gallmann, and U. Keller, *Optica* **1**, 343 (2014).
 - [2] P. Eckle, A. N. Pfeiffer, C. Cirelli, A. Staudte, R. Dörner, H. G. Muller, M. Büttiker, and U. Keller, *Science* **322**, 1525 (2008).
 - [3] P. Eckle, M. Smolarski, F. Schlup, J. Biegert, A. Staudte, M. Schöffler, H. G. Muller, R. Dörner, and U. Keller, *Nat. Phys.* **4**, 565 (2008).
 - [4] O. Kullie, *Phys. Rev. A* **92**, 052118 (2015), arXiv:1505.03400v2.
 - [5] U. Satya Sainadh, H. Xu, X. Wang, Atia-Tul-Noor, W. C. Wallace, N. Douguet, A. W. Bray, I. Ivanov, K. Bartschat, A. Kheifets, R. T. Sang, and I. V. Litvinyuk, *Nature* **568**, 75 (2019), arXiv:1707.05445 (2017).
 - [6] O. Kullie, *J. Phys. Commun.* **2**, 065001 (2018).
 - [7] Y. Aharonov and B. Reznik, *Phys. Rev. Lett.* **84**, 1368 (2000).
 - [8] Gennaro Auletta, M. Fortunato, and G. Parisi, *Quantum Mechanics* (Cambridge University Press, 2009).
 - [9] S. Augst, D. Strickland, D. D. Meyerhofer, S. L. Chin, and J. H. Eberly, *Phys. Rev. Lett.* **63**, 2212 (1989).
 - [10] S. Augst, D. D. Meyerhofer, D. Strickland, and S. L. Chin, *J. Opt. Soc. Am. B* **8**, 858 (1991).
 - [11] L. V. Keldysh, *Zh. eksp. teor. Fiz.* **47**, 1945 (1964), [English translation: 1965, *Soviet Phys. JETP*, **20**, 1307].
 - [12] H. R. Reiss, *Phys. Rev. A* **22**, 1786 (1980).
 - [13] F. H. M. Faisal, *J. Phys. B* **6**, L89 (1973).
 - [14] H. R. Reiss, *Phys. Rev. A* **54**, R1765 (1996).
 - [15] H. R. Reiss, *Phys. Rev. A* **82**, 023418 (2010).
 - [16] H. R. Reiss, *Arxiv.1810.12106v4*, (2019).
 - [17] C. Hofmann, A. S. Landsman, and U. Keller, *J. Mod. Opt.* **66**, 1052 (2019), open access.
 - [18] N. B. Delone and V. P. Krainov, *Phys.-Usp.* **41**, 469 (1998).
 - [19] I. Yu. Kiyani and V. P. Krainov, *Soviet Phys. JETP* **74**, 429 (1991).
 - [20] Ossama Kullie, *Journal of Physics B: Atomic, Molecular and Optical Physics* **49**, 095601 (2016).
 - [21] O. Kullie, *Ann. of Phys.* **389**, 333 (2018), arXiv:1701.05012.
 - [22] O. Kullie, *Qunat. Rep.* **2**, 233 (2020).
 - [23] H. G. Winful, *Phys. Rev. Lett.* **91**, 260401 (2003).
 - [24] Ivanov I. A. and A. S. Keifets, *Phys. Rev. A* **89**, 021402 (2014).
 - [25] N. B. Delone and V. P. Krainov, *Multiphoton Processes in Atoms*, 2nd ed. (Springer-Verlag Berlin, 2000).
 - [26] C. Hofmann, private communication.
 - [27] A. M. Perelomov, V. S. Popov, and M. V. Terent'ev, *Zh. eksp. teor. Fiz.* **50**, 1393 (1966), [*Soviet Phys. JETP*, **23**, 924 (1966)].
 - [28] M. Klaiber, K. Z. Hatsagortsyan, and C. H. Keitel, *Phys. Rev. Lett.* **114**, 083001 (2015).
 - [29] D. D. Meyerhofer, *IEEE J. Quantum Electron.* **33**, 1935 (1997).
 - [30] E. Clementi and D. L. Raimondi, *J. Chem. Phys.* **38**, 2686 (1963).
 - [31] R. Boge, C. Cirelli, A. S. Landsman, S. Heuser, A. Ludwig, J. Maurer, M. Weger, L. Gallmann, and U. Keller, *Phys. Rev. Lett.* **111**, 103003 (2013).
 - [32] O. Kullie, Nonadiabatic attoclock and Above-threshold ionization. The multiphoton ionization in Ar, Kr atoms. Work in preparation.
 - [33] O. Kullie, *Mathematics* **6** (2018).
 - [34] M. Y. Ivanov, M. Spanner, and O. Smirnova, *J. Mod. Opt.* **52**, 165 (2005).
 - [35] M. Klaiber and J. S. Briggs, *Phys. Rev. A* **94**, 053405 (2016).
 - [36] J. S. Briggs and J. H. Macek, *Adv. At. Mol. Opt. Phys.* **28**, 1 (1990).
 - [37] Joseph H. Eberly, *Phys. Rev. Lett.* **15**, 91 (1965).
 - [38] Carver Mead, *Collective Electrodynamics: Quantum Foundations of Electromagnetism* (MIT Press, Cambridge, Mass., 2000) see also C. Mead, the Nature Of Light What Are Photons, www.cns.caltech.edu.

- [39] E. E. Serebryannikov and A. M. Zheltikov, Phys. Rev. Lett. **116**, 123901 (2016).